IOPscience iopscience.iop.org

Home Search Collections Journals About Contact us My IOPscience

Direct writing on graphene ‘paper’ by manipulating electrons as ‘invisible ink’

This article has been downloaded from IOPscience. Please scroll down to see the full text article.

2013 Nanotechnology 24 275301

(http://iopscience.iop.org/0957-4484/24/27/275301)

View the table of contents for this issue, or go to the journal homepage for more

Download details:
IP Address: 101.5.154.35
The article was downloaded on 07/06/2013 at 11:54

Please note that terms and conditions apply.

Nanotechnology **24** (2013) 275301 (6pp) doi:10.1088/0957-4484/24/27/275301

Direct writing on graphene 'paper' by manipulating electrons as 'invisible ink'

Wei Zhang[1], Qiang Zhang[2], Meng-Qiang Zhao[2] and Luise Theil Kuhn[1]

[1] Department of Energy Conversion and Storage, Technical University of Denmark, Risø Campus, Frederiksborgvej 399, DK-4000 Roskilde, Denmark
[2] Beijing Key Laboratory of Green Chemical Reaction Engineering and Technology, Department of Chemical Engineering, Tsinghua University, Beijing 100084, People's Republic of China

E-mail: wzha@dtu.dk, phdweizhang@gmail.com and zhang-qiang@mails.tsinghua.edu.cn

Received 8 February 2013, in final form 2 May 2013
Published 7 June 2013
Online at stacks.iop.org/Nano/24/275301

Abstract
The combination of self-assembly (bottom up) and nano-imprint lithography (top down) is an efficient and effective way to record information at the nanoscale by writing. The use of an electron beam for writing is quite a promising strategy; however, the 'paper' on which to save the information is not yet fully realized. Herein, graphene was selected as the thinnest paper for recording information at the nanoscale. In a transmission electron microscope, *in situ* high precision writing and drawing were achieved on graphene nanosheets by manipulating electrons with a 1 nm probe (probe current $\sim 2 \times 10^{-9}$ A m^{-2}) in scanning transmission electron microscopy (STEM) mode. Under electron probe irradiation, the carbon atom tends to displace within a crystalline specimen, and dangling bonds are formed from the original sp^2 bonding after local carbon atoms have been kicked off. The absorbed random foreign amorphous carbon assembles along the line of the scanning direction induced by secondary electrons and is immobilized near the edge. With the ultralow secondary electron yield of the graphene, additional foreign atoms determining the accuracy of the pattern have been greatly reduced near the targeting region. Therefore, the electron probe in STEM mode serves as invisible ink for nanoscale writing and drawing. These results not only shed new light on the application of graphene by the interaction of different forms of carbon, but also illuminate the interaction of different carbon forms through electron beams.

(Some figures may appear in colour only in the online journal)

1. Introduction

Drawing and/or writing is a powerful way to record information. Recently, manipulation of matter on an atomic and molecular scale became feasible with emerging nanotechnology. Resist-based lithography by light, ultraviolet, x-ray and electron irradiation is widely employed in the microelectronic industry via top-down methods [1]. However, its resolution is highly restricted by the diffraction effect. The other route to organize the atoms or molecules from the bottom up is quite promising, but the controllability is not yet satisfactory. For instance, a femtosecond laser can create powerful imprinting, but the resolution is limited to microscale areas [2]. The combination method, based on self-assembly (bottom up) and nano-imprint lithography (top down), can meet the requirement of nanoscale writing.

Among various sources for writing, electrons are a well-controllable tool for modifying or engineering the properties of different materials at the nanoscale. With the rapid development of electron microscopy with the field-emission electron gun, localized electron probes can be used for electron-induced processes on the nanometer and subnanometer scales [3–5]. New bond formation or dissociation can be feasible when the electrons are injected or removed. Electron-induced deposition is a facile way to grow nanowires or nanorods [6], contacting carbon nanotubes [7, 8] and fabricating complex arbitrarily shaped nanostructures [9–11]. As a result, bottom-up assembly can be well mediated by a top-down electron beam, which is

 © 2013 IOP Publishing Ltd Printed in the UK & the USA

resistless and usable *in situ* and has a resolution of less than 5 nm [1, 12]. The use of an electron beam for writing is a quite promising strategy; however, the 'paper' on which to record the information is not fully developed yet.

Graphene is known as an individual single layer or a few layers of a two-dimensional sp^2-bonded carbon sheet, i.e. a single layer composed of a hexagonal network of carbon atoms [13]. Graphene has the distinct characteristic of being the thinnest material known [14]. Graphene is a flat and uniform sheet and is therefore feasible as the thinnest paper. It can be made by mechanical exfoliation [13], chemical vapor deposition (CVD) [15] or liquid-phase exfoliation [16], as well as reduction of graphene oxide [17, 18]. Tailoring the properties of graphene and its related nanoarchitectures heavily depends on both the crystallographic orientation and the actual atomic structure of the edges, which involves quite challenging processing [19]. The carbon species in graphene are sensitive to a variety of irradiation effects, including knock-on displacements, electronic excitations, radiolysis and radiation-induced diffusion. Therefore, an electron beam is a very effective tool for probing the interaction between electrons and carbon atoms on amorphous carbon [20] and graphene [21–23]. For instance, the irradiation of amorphous carbon with a 100 or 200 keV electron beam induces the formation of sp^2 carbon onions [24]. By adjusting the electron beam mode and the dose for electron acceleration energies, the deposited amorphous carbon can be converted into graphene via catalyst-free fabrication [25]. Graphene nanopores can shrink or expand under electron beam irradiation by direct thermal heating dependent on the ratio of the nanopore diameter to membrane thickness [26]. The nanoholes etched under an electron beam at room temperature in graphene sheets are shown to heal spontaneously by filling up with either nonhexagonal, graphene-like or perfect two-dimensional hexagonal structures [27]. Furthermore, the exfoliated few-layer graphene has been used as a support for the early growth phase by electron beam induced deposition in order to achieve nanoscale writing [28]. Stimulated by the fact that graphene can be used as a template for the manipulation of the tip of atomic force microscope in a hydrogen atmosphere [29], and that electron beam can achieve sculpting in graphene [30], here direct writing and drawing with high precision (a few nanometers in one dimension) is achieved on graphene by manipulating electrons in a transmission electron microscope (TEM). We demonstrate that amorphous carbon could be selected for position- and size-controllable deposition on the target area of the graphene using electrons as invisible 'ink'.

2. Experiments

The synthesis of graphene was carried out using high-temperature catalytic chemical vapour deposition (CVD) on layered double hydroxide catalysts similar to our previous report [31]. After graphene deposition, the as-obtained products were treated by aqueous HCl solution at 80 °C for 3 h and subsequent aqueous NaOH solution at 150 °C for 6 h to remove the residual catalysts. The as-obtained graphene nanosheets with a diameter of about 2 μm and a thickness of about 1 nm were obtained by filtration, washing and freeze-drying for further characterization.

The graphene was dispersed in ethanol by sonicating for 30 min. One drop was taken onto the holey carbon film supported on a copper grid, followed by 10 min heating on the heating stage at 120 °C. The use of a holey carbon film for support has also been reported in the literature [28, 30].

A JEOL JEM-3000F microscope equipped with a field-emission gun, operated at 300 kV, was employed for TEM observation and analysis. An energy dispersive x-ray (EDX) microanalysis detector with an ultra-thin window was used to conduct chemical analysis of samples in scanning transmission electron microscopy (STEM) mode, including EDX spectrum elemental maps and line scan profiles. The beam-deflection capability of the EDX system has been used to 'write' the letters on the graphene. The STEM image was initially displayed for imaging optimization on a cathode ray tube screen. Subsequently the image was acquired by use of a second system consisting of INCA software (Oxford Instruments, UK). The 1 nm probe was used with a probe current $\sim 2 \times 10^{-9}$ A m^{-2} in STEM mode. The minimum spot size 9 was applied in STEM mode.

3. Results and discussion

The graphene nanosheets were distributed on a holey carbon film. As shown in figure 1(a), the graphene can be clearly visualized. The imaging contrast was enhanced by high angle annular dark field (HAADF) imaging in figure 1(b). The graphene flakes were closely packed against each other, and their edges were identified (indicated by arrows shown in figure 1(b)). The high-resolution TEM image shown as figure 1(c) indicates that the graphene flakes are almost single layer, judging by the distinct edge contrast (see the arrow). Ripples and twists exist in the sheet. The chemical composition of the graphene was 98 wt% C and 2 wt% O, determined by the EDX analysis.

The single layer region of the graphene was selected as the 'paper' for electron 'ink' writing. As shown in figure 2(a), one layer of graphene and two layers are clearly identified by bright-field STEM imaging. Therefore, the fine probe in the STEM mode is sufficient to precisely pattern the graphene. With approximately 60 s per scanned line, when the EDX counts of carbon increased from zero to 60 (as illustrated in figure 2(b)), the bold (dense) letter 'N' and symbol 'Λ' were successfully written on the single layer graphene. The font size (width of stroke lines) is 5 nm for their main part. In fact, we found that the writing action started once the number of EDX counts started to accumulate. When there are fewer than 10 counts it is difficult to visualize the writing trace. The aforementioned condition is quite suitable for optimum writing on a single graphene sheet. Using the same EDX counts, a regular (delicate and pretty) 'и' (N after flip horizontal) with a font size of 2–3 nm for the main part occurred on the double layer graphene. Clearly the HAADF STEM image (figure 2(c)) offers the better contrast in comparison with the bright field STEM

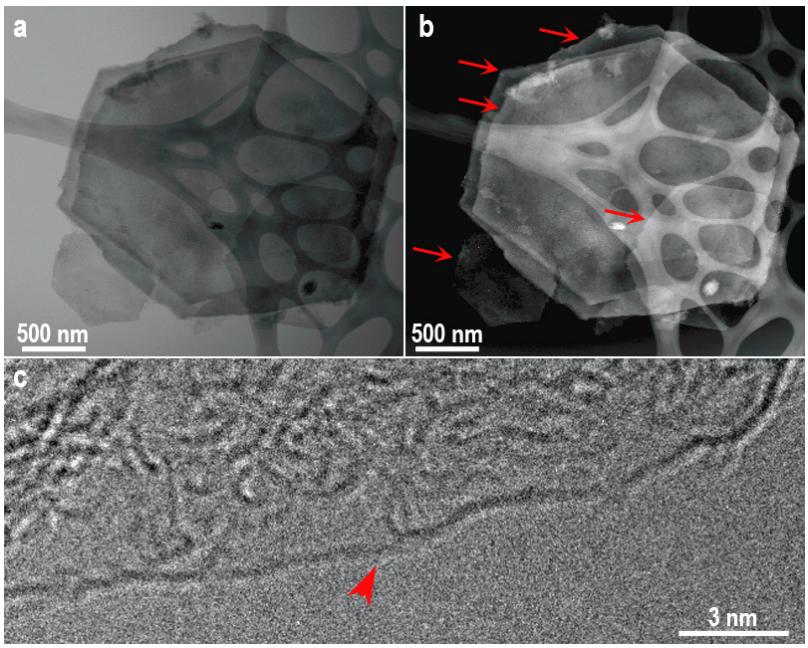

Figure 1. (a) Bright field (BF) and (b) HAADF STEM images of a few layers of graphene. (c) High-resolution TEM image of a local region.

image. Through EDX elemental mapping (see the eclipsed area for the local bold bottom-left part of Λ), more carbon atoms were deposited by virtue of electron manipulation. A high-resolution TEM image of the 'written' graphene is shown in figure 2(d) (see the arrow).

Not only direct writing, but also facile drawing of various shapes can be realized by electron manipulated carbon deposition. Figures 3(a) and (b) show the target area 'A' from the blank graphene 'paper' to the filling with a quadrilateral or triangular region (figure 3(c)). The shape of the target area can be well delineated by using the pre-defined shapes to acquire the EDX spectrum (in INCA software).

In comparison with the use of other intense electron beams (TEM and high-resolution TEM) with graphene, our application with a focused electron beam is very promising because the STEM mode provides a high precision probe-targeting position [32], which greatly reduces irradiation damage from the electron beam to adjacent regions. In order to remove carbon atoms from the graphene sheet by direct knock-on collision, the minimum incident electron beam energy is 86 keV [33]. Such elastic scattering represents electrostatic deflection of incoming electrons by the Coulomb field of each atomic nucleus. Herein, the graphene sample was manipulated by a 300 keV electron beam. Such high energy electrons break the local carbon–carbon bonding sp^2 in the graphene. On one hand, the carbon atom is preferred for displacement within a crystalline specimen; on the other hand, the electron beam sputters the carbon atoms out of their matrix. Such scattering phenomena can be easily detected when observing single or a few layer graphene. The high angle elastic scattering (here in STEM mode) occurred on an atom at the surface of a specimen, and the surface atom leaves the specimen and enters the vacuum. As shown in figure 4, dangling bonds were formed from the original sp^2 bonding after local carbon atoms were kicked off. The dangling bonds can attract carbon species from the vacuum onto the surface. Such absorbed random foreign amorphous carbon is used to stabilize the edge [34]. These foreign carbon species assemble along the line scanning direction and are immobilized near the edge. Meanwhile, the Coulomb interaction of incoming electrons with the atomic electrons that surround each nucleus gives rise to inelastic scattering. This leads to the emission of x-rays (here EDX for elemental analysis). The induced radiolysis effects also result in many defects and local disorder in the graphene. It is known that when using a gas precursor in the electron beam induced deposition technique secondary electrons play a critical role in a variety of nanofabrication processes [35–37]. Therefore, the carbon deposition occurred due to secondary electrons.

It is very difficult to characterize the line edge roughness of graphene (such as graphene nanoribbon with zig-zag or armchair edge) by a routine TEM without a spherical aberration corrector; therefore, the line edge roughness of graphene is assumed to be correlated with the amorphous carbon/sp^2 carbon interface. Secondary electrons generated in the graphene have an escape length of the order of the graphene thickness. Because of the ultralow secondary electron yield of the graphene [38], more additional foreign carbon atoms influencing the accuracy of the pattern have been largely reduced near the targeting region. Such a reduction in line edge roughness increases the efficiency of writing. Specimen drift during writing also induces the roughness of carbon/carbon interface, which should be minimized during the nanopattern fabrication process. As shown in figure 2(d), the width of the straight written line can be quite uniform at only 2 nm. Such a width of the nanopattern on graphene paper is comparable with the probe size.

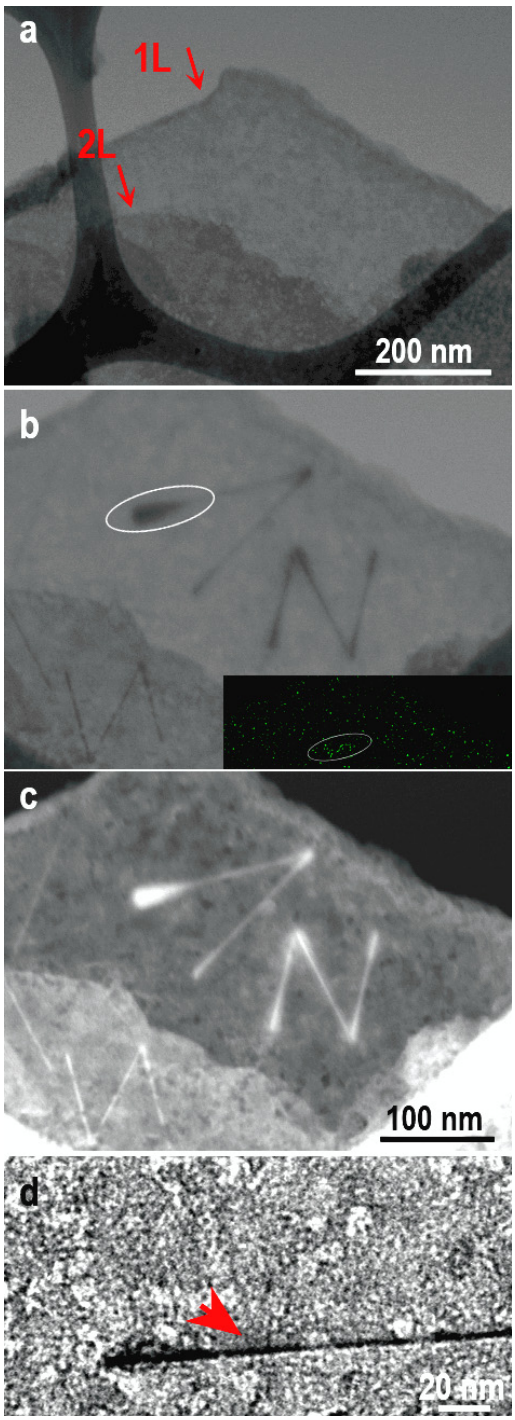

Figure 2. (a) Bright field STEM image of graphene. (b) Bright field and (c) HAADF STEM images of the counterpart after writing. The inset in (b) shows the carbon elemental map of the writing pattern marked by the eclipsed area. (d) High-resolution TEM image of local region after writing.

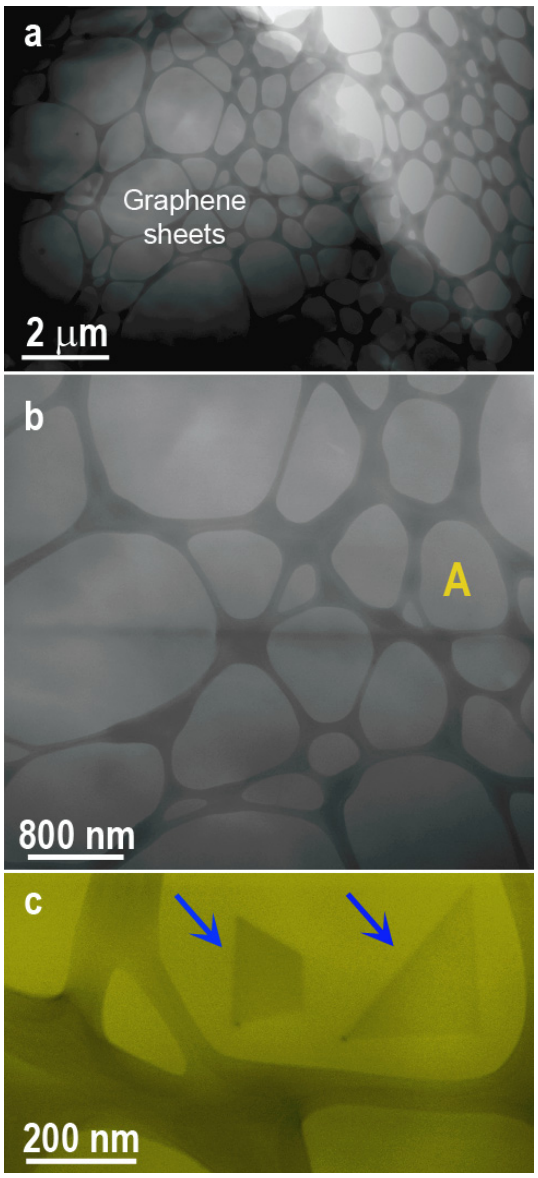

Figure 3. (a), (b) Bright field STEM images of multi-layered graphene. The target area was labeled as 'A' on the graphene 'paper'. (c) Bright field STEM images of the area after shape drawing. The false color processing was done in INCA software to enhance the contrast for the drawing shapes.

With continuous absorption and the complicated scenarios of electron–atom interaction, carbon deposition continues to increase with scanning time, crosslinking to form amorphous carbon lines along the scanning direction. Therefore, direct writing and drawing on graphene can be realized using controllable carbon deposition. Writing can be conducted in both bright field and HAADF STEM modes. In contrast to the bright field image, the HAADF STEM mode gives enhanced writing contrast as it is sensitive enough to detect a small local change in carbon concentration along the damaged graphene.

STEM writing can be performed from several to tens of seconds, depending on how pristine the sample is and the electron beam current. The electron beam can be tuned in the following aspects: (1) with a larger spot size, the probe current increased, which contributes to the writing efficiency; (2) lowering the magnification enlarges the writing scope at the cost of sacrificing the writing resolution.

Currently there are several emerging approaches for writing on graphene-based materials, e.g. using a catalytic atomic force microscope tip to write on graphene oxide [29], using a Cs-corrected electron beam to achieve sculpting of

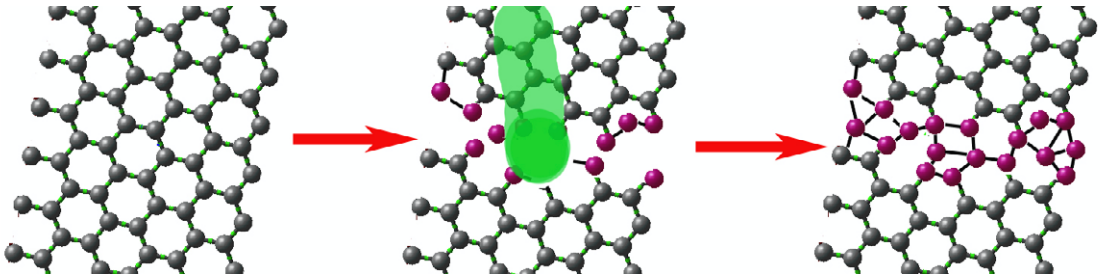

Figure 4. Schematic illustration of the direct writing by the electron beam on graphene 'paper'. Some of the sp^2 carbon atoms in the graphene were kicked off, and external carbon atoms deposited on the dangling bonds.

graphene [30], and electron beam induced deposition on graphene by applying a metalorganic gas precursor [28]. Herein the essence of our work lies in a direct writing of sub-10 nm lines on graphene with STEM. It is not necessary to choose any high-end instrument, and a routine microscope can be utilized to easily perform direct wiring on the graphene sheet, which is therefore a promising nanotechnology to pattern nanostructures for electronic and sensor applications.

4. Concluding remarks

Direct high precision microscopic writing on graphene was achieved through an EDX line scan with 1 nm probe (probe current $\sim 2 \times 10^{-9}$ A m^{-2}) in STEM mode, by the dangling bonds from the local broken sp^2 bonds absorbing and incorporating more carbon atoms in the vacuum and on the surface. The formation processes have been elucidated through STEM related microanalysis that probes direct growth of carbon along the electron scan tracing. The graphene preserved its morphology after writing/drawing. It is noted that other hydrocarbon contamination can be occasionally induced on some thin films irradiated under an electron beam. Herein position- and size-controllable writing on graphene in a high-vacuum environment can be easily achieved. These results not only shed new light on an application of graphene concerning the interaction of different forms of carbon but also illuminate the interaction of forms of carbon through an electron beam.

Acknowledgments

The authors have received much help from the referees' insightful comments and valuable suggestions. Q Zhang acknowledges support from the National Basic Research Program of China (973 Program, 2011CB932602).

References

[1] Vieu C, Carcenac F, Pepin A, Chen Y, Mejias M, Lebib A, Manin-Ferlazzo L, Couraud L and Launois H 2000 Electron beam lithography: resolution limits and applications *Appl. Surf. Sci.* **164** 111–7

[2] Zhang Y L, Guo L, Wei S, He Y Y, Xia H, Chen Q D, Sun H B and Xiao F S 2010 Direct imprinting of microcircuits on graphene oxides film by femtosecond laser reduction *Nano Today* **5** 15–20

[3] Zhang B S, Wang D, Zhang W, Su D S and Schlogl R 2011 Structural dynamics of low-symmetry Au nanoparticles stimulated by electron irradiation *Chem.—Eur. J.* **17** 12877–81

[4] Zhang W, Zhang B S, Wolfram T, Shao L D, Schlogl R and Su D S 2011 Probing a redox behavior of TiO_2/SBA-15 supported V_xO_y catalyst using an electron beam in a 200 kV transmission electron microscope *J. Phys. Chem.* C **115** 20550–4

[5] Van Tendeloo G, Bals S, Van Aert S, Verbeeck J and Van Dyck D 2012 Advanced electron microscopy for advanced materials *Adv. Mater.* **24** 5655–75

[6] Zhang W, Shimojo M and Furuya K 2008 Effect of dynamic precursor gas pressure on growth behavior of amorphous Si–C–O nanorods by electron beam-induced deposition *J. Mater. Sci.* **43** 2069–71

[7] Gopal V, Radmilovic V R, Daraio C, Jin S, Yang P D and Stach E A 2004 Rapid prototyping of site-specific nanocontacts by electron and ion beam assisted direct-write nanolithography *Nano Lett.* **4** 2059–63

[8] Wang Y G, Wang T H, Lin X W and Dravid V P 2006 Ohmic contact junction of carbon nanotubes fabricated by *in situ* electron beam deposition *Nanotechnology* **17** 6011–5

[9] Zhang W, Liu Z Q and Furuya K 2008 Fabrication and characterization of cellular iron nanocrystalline film *Nanotechnology* **19** 135302

[10] Steenackers M, Jordan R, Kuller A and Grunze M 2009 Engineered polymer brushes by carbon templating *Adv. Mater.* **21** 2921–5

[11] Mackus A J M, Dielissen S A F, Mulders J J L and Kessels W M M 2012 Nanopatterning by direct-write atomic layer deposition *Nanoscale* **4** 4477–80

[12] Botman A, Mulders J J L and Hagen C W 2009 Creating pure nanostructures from electron-beam-induced deposition using purification techniques: a technology perspective *Nanotechnology* **20** 372001

[13] Novoselov K S, Geim A K, Morozov S V, Jiang D, Zhang Y, Dubonos S V, Grigorieva I V and Firsov A A 2004 Electric field effect in atomically thin carbon films *Science* **306** 666–9

[14] Soldano C, Mahmood A and Dujardin E 2010 Production, properties and potential of graphene *Carbon* **48** 2127–50

[15] Li X S *et al* 2009 Large-area synthesis of high-quality and uniform graphene films on copper foils *Science* **324** 1312–4

[16] Coleman J N 2009 Liquid-phase exfoliation of nanotubes and graphene *Adv. Funct. Mater.* **19** 3680–95

[17] Chen C M, Zhang Q, Yang M G, Huang C H, Yang Y G and Wang M Z 2012 Structural evolution during annealing of thermally reduced graphene nanosheets for application in supercapacitors *Carbon* **50** 3572–84

[18] Pei S F and Cheng H M 2012 The reduction of graphene oxide *Carbon* **50** 3210–28 and references therein

[19] Biro L P, Nemes-Incze P and Lambin P 2012 Graphene: nanoscale processing and recent applications *Nanoscale* **4** 1824–39
[20] Zhang W 2013 Revealing the 1 nm/s extensibility of nanoscale amorphous carbon in a scanning electron microscope *Scanning* **35** doi:10.1002/sca.21059
[21] Meyer J C *et al* 2012 Accurate measurement of electron beam induced displacement cross sections for single-layer graphene *Phys. Rev. Lett.* **108** 196102
[22] Kotakoski J, Santos-Cottin D and Krasheninnikov A V 2012 Stability of graphene edges under electron beam: equilibrium energetics versus dynamic effects *ACS Nano* **6** 671–6
[23] Fischbein M D and Drndic M 2008 Electron beam nanosculpting of suspended graphene sheets *Appl. Phys. Lett.* **93** 113107
[24] Banhart F and Ajayan P M 1996 Carbon onions as nanoscopic pressure cells for diamond formation *Nature* **382** 433–5
[25] Börrnert F, Avdoshenko S M, Bachmatiuk A, Ibrahim I, Büchner B, Cuniberti G and Rümmeli M H 2012 Amorphous carbon under 80 kV electron irradiation: a means to make or break graphene *Adv. Mater.* **24** 5630–5
[26] Xu T, Yin K B, Xie X, He L B, Wang B J and Sun L T 2012 Size-dependent evolution of graphene nanopores under thermal excitation *Small* **8** 3422–6
[27] Zan R, Ramasse Q M, Bangert U and Novoselov K S 2012 Graphene reknits its holes *Nano Lett.* **12** 3936–40
[28] van Dorp W F, Zhang X, Feringa B L, Wagner J B, Hansen T W and De Hosson J T M 2011 Nanometer-scale lithography on microscopically clean graphene *Nanotechnology* **22** 505303
[29] Zhang K, Fu Q, Pan N, Yu X, Liu J, Luo Y, Wang X, Yang J and Hou J 2012 Direct writing of electronic devices on graphene oxide by catalytic scanning probe lithography *Nature Commun.* **3** 1194
[30] Börrnert F, Fu L, Gorantla S, Knupfer M, Buchner B and Rummeli M H 2012 Programmable sub-nanometer sculpting of graphene with electron beams *ACS Nano* **6** 10327–34
[31] Zhao M Q, Liu X F, Zhang Q, Tian G L, Huang J Q, Zhu W C and Wei F 2012 Graphene/single-walled carbon nanotube hybrids: one-step catalytic growth and applications for high-rate Li–S batteries *ACS Nano* **6** 10759–69
[32] Muller D A 2009 Structure and bonding at the atomic scale by scanning transmission electron microscopy *Nature Mater.* **8** 263–70
[33] Zobelli A, Gloter A, Ewels C P, Seifert G and Colliex C 2007 Electron knock-on cross section of carbon and boron nitride nanotubes *Phys. Rev.* B **75** 245402
[34] Jia X T, Campos-Delgado J, Terrones M, Meunier V and Dresselhaus M S 2011 Graphene edges: a review of their fabrication and characterization *Nanoscale* **3** 86–95
[35] Randolph S J, Fowlkes J D and Rack P D 2006 Focused, nanoscale electron-beam-induced deposition and etching *Crit. Rev. Solid State* **31** 55–89
[36] Utke I, Hoffmann P and Melngailis J 2008 Gas-assisted focused electron beam and ion beam processing and fabrication *J. Vac. Sci. Technol.* B **26** 1197–276
[37] Zhang W, Shimojo M, Takeguchi M, Che R C and Furuya K 2006 Generation mechanism and *in situ* growth behavior of alpha-iron nanocrystals by electron beam induced deposition *Adv. Eng. Mater.* **8** 711–4
[38] Luo J, Tian P, Pan C T, Robertson A W, Warner J H, Hill E W and Briggs G A D 2011 Ultralow secondary electron emission of graphene *ACS Nano* **5** 1047–55